Character of F core excitons in alkali fluorides studied by resonant Auger spectroscopy

H. Aksela, E. Kukk, S. Aksela, A. Kikas,* and E. Nõmmiste*
Department of Physics, University of Oulu, SF-90570 Oulu, Finland

A. Ausmees*
Department of Physics, University of Uppsala, Box 530, S-75121 Uppsala, Sweden

M. Elango
Department of Experimental Physics and Technology, Tartu University, Ülikooli 18, EE2400 Tartu, Estonia and Institute of Physics, Estonian Academy of Sciences, Riia 142, EE2400 Tartu, Estonia
(Received 6 July 1993)

The resonant KLL Auger spectra of fluorine have been measured from *in situ* evaporated films of LiF, NaF, and KF using synchrotron radiation of the MAX I storage ring, Lund, Sweden. The measured Auger electron spectra show strong enhancement at the F 1s absorption edge. New Auger peaks appear at excitation energies below the photoionization threshold. These peaks are shifted to higher kinetic energies in comparison with the normal Auger spectra. They correspond to the excitation of the core excitons followed by the resonant Auger transitions where the excited electron remains as a screening spectator electron during the Auger decay. With the aid of resonant features we have identified the regions of different character inside the comparatively wide absorption peaks. The atomic picture and the comparison with the isoelectronic Ne atom have been applied successfully in the interpretation of the spectra of F.

I. INTRODUCTION

An inner shell electron can be excited by photoabsorption to a bound state below the ionization threshold. The corresponding resonant photoabsorption peaks may be well resolved, as usually is the case for atoms, or overlapped with the features of the main absorption edge. In the deexcitation by an Auger transition the electron may remain as a screening electron both in the initial and final states (spectator Auger decay). This causes an increase in the energy of the outgoing Auger electron compared with the normal Auger decay without the presence of the excited electron. Within the simplest picture (strict spectator model) the spectator Auger spectrum is just a shifted replica of the normal Auger spectrum. The coupling between the spectator electron and the electrons involved in the decay, however, causes additional splitting that can be resolved in high resolution atomic studies.[1] The spectator electron may also shake up or down or off during the Auger decay, resulting in structures that are shifted in comparison with the spectator ones to the lower or higher kinetic energies. If the excited electron takes part in the Auger decay, the energy of the final state will be the same as for single hole states created by photoemission. The outgoing electron is then indistinguishable by its energy from the photoelectrons. The existence of participator Auger decay is observable as resonant enhancement of the photoline intensities at the photon energies corresponding to the resonant photoabsorption peaks.

It is known that in the core level absorption spectra of insulating solids and semiconductors there are also sharp peaks due to core excitons below the ionization threshold. There is a close analogy between the core-excited states of atoms and core excitons in solids. In both cases the excited electron is bound to the inner hole state by electrostatic forces, but in solids this electron can be localized in much bigger volume that contains much more than one atom.

Resonant Auger spectroscopy provides a new and powerful method to study the core excitons in ionic solids.[2,3] Concerning the fluorides, both the participator and spectator decay channels have been observed to appear in the Auger spectra of CaF_2 near the Ca 2p absorption edge.[2] Close to the F 1s absorption edge the deexcitation was found to take place only via the spectator Auger decay channel. On the basis of this finding it was assumed that at the Ca 2p edge the excited electron is localized on the Ca ion, whereas at the F 1s edge it is not localized directly on the same fluorine ion, where the core hole exists. This picture is consistent with the idea that the states near the bottom of the conduction band originate genetically from cations and therefore electrons excited to these states cannot be localized on anions.

Consequently there is a difference between the core excitons below the cation and anion edges in ionic crystals. In the case of cation excitons the excited electron remains localized in the vicinity of the ion with core hole. The absorption and Auger spectra of cations in solids and corresponding free atoms are quite similar. In the case of anion excitons the configuration with an additional electron is not as stable as in free atoms and in solids the

excited electron is localized loosely around the ion with an inner hole. In this case the core exciton is similar to the optical exciton, for which the mean distance between the valence hole and bound excited electron is some lattice constants.

In atomic studies the core-excited states have been found to decay predominantly via spectator Auger decay.[4] For instance, for the $1s^1 2s^2 2p^6 3p$ excited state of Ne the calculated participator decay rate was 0.023×10^{-3} a.u. whereas the total decay rate was 10.357×10^{-3} a.u.[5] Only in the case where the electron is excited to a collapsing $3d$ or $4f$ orbital has the participator decay channel been found to play a prominent role. The absence of participator transitions are thus not, on the basis of atomic studies, sufficient to prove the delocalization of the excitonic state in solids.

In order to investigate in detail the photoabsorption and Auger decay processes near the $1s$ edge of F we have measured and analyzed the resonant Auger spectra of LiF, NaF, and KF. The results have been used to reveal a better understanding of the nature of core excitons in alkali fluorides.

II. EXPERIMENTAL DETAILS AND RESULTS

The measurements were performed using synchrotron radiation at the MAX-LAB in Lund. The Zeiss SX-700 monochromator and Scienta SES-200 hemispherical electron energy analyzer at the beam line 22 were used.[6] The sample films were prepared by thermal evaporation *in situ* from a molybdenum boat onto polished stainless steel substrates in a vacuum below 5×10^{-7} torr. The film thickness (about 100 Å) and the evaporation rate (several Å/s) were controlled by a quartz crystal monitor. The vacuum in the experimental chamber was typically 2×10^{-10} torr during the measurements. No sample charging effects greater than 0.1 eV were observed in the experiments.

The photoabsorption was studied by measuring the total electron yield spectra, since they are known to reproduce well the absorption spectra also in the case of ionic solids. The photon energy resolution, used in the course of measurements, was limited by the need to get good statistics on the Auger spectra in a reasonable time. For the SX-700 monochromator of beam line 22, the photon bandwidth is known to be about 1 eV at 700 eV photon energy with a 1221 l/mm grating and 50 μm exit slit used. Under these experimental conditions the width of the fluorine $1s$ photoline was observed to be 1.7 eV. The photon energy calibration was done on the basis of the kinetic energy difference of the photoelectron lines created by the first and the second order diffracted light. No absolute electron energy calibration was done for the spectra, as only the shifts of Auger lines are considered here.

The deexcitation processes were studied by recording the electron spectra at selected mean photon energies. The kinetic energy resolution of the electron spectrometer was 0.2 eV during the recordings.

A. LiF

The photoabsorption spectrum of LiF shown as inset in Fig. 1 is in good agreement with the spectra reported earlier[7,8] despite the lower photon energy resolution. The spectrum displays a clear shoulder below the absorption maximum which is located at 692.5 eV. The shoulder is better resolved in a high resolution measurement reported by Nakai *et al.*[7] The labeled arrows in the inset denote photon energies for which the deexcitation spectra were recorded. These electron spectra are presented in Fig. 1 together with a spectrum taken at nonresonant excitation energy (800 eV). The nonresonant spectrum, indicated by N in Fig. 1, reveals a typical structure of the KLL Auger transitions, consisting of the clearly separated single $KL_1L_1(^1S)$ line, followed by the $KL_1L_{23}(^1P)$ and $KL_1L_{23}(^3P)$ lines in the middle part and by the $KL_{23}L_{23}(^1S)$ and the dominating $KL_{23}L_{23}(^1D)$ Auger lines around 650–655 eV. The energy separation between the ^1S and ^1D lines of the $KL_{23}L_{23}$ group was found from curve fitting to be 3.0 eV. The splitting between the ^1S and ^1D lines was kept constant when fitting the resonance features discussed below.

Our spectra were found to contain a weak structure, which originates from the KLL Auger transitions, also at the photon energies far below the F $1s$ absorption edge. This structure is caused by the scattered high energy photons. The number of scattered photons increases with increasing photon energy. For example, in the case of LiF the branching ratio between the main $KL_{23}L_{23}$ peak created by scattered photons and the valence band

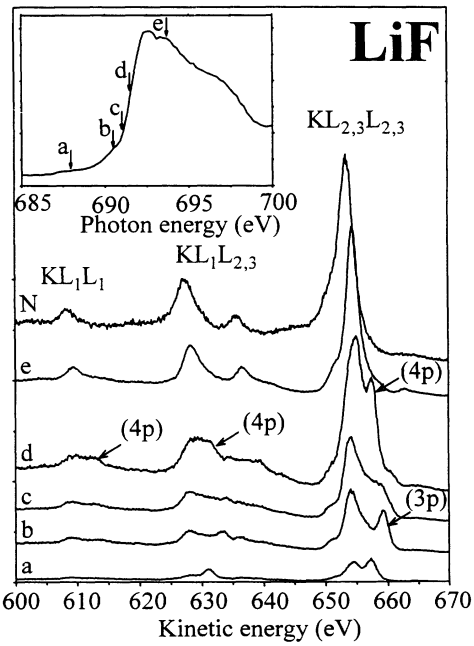

FIG. 1. Normal (denoted by N) and resonant Auger spectra of LiF. Inset shows the total electron yield spectrum of LiF at the F K edge. Labels a–e indicate the mean photon energies where the electron spectra were recorded. The normal Auger electron spectrum was taken at $h\nu = 800$ eV.

photoelectron spectrum grew from 1/3 to 2/3 when the exciting photon energy was changed from 650 to 670 eV. These Auger peaks are replaced by shifted and more intense peaks at the photon energies of Fig. 1. The new peaks are shifted about 1 eV to higher kinetic energy. These peaks result also from the $KL_{23}L_{23}$ Auger transitions, which are excited by photons with energy near to the absorption maxima. Kinetic energies of the ^1D lines are given in Table I.

The resonant Auger spectra of LiF, labeled by *b* and *d* in Fig. 1, show strong differences from the normal one. An addititional peak seems to appear in the $KL_{23}L_{23}$ Auger spectrum, when the photon energy is tuned to the position *b* shown in the inset. A detailed fit of the spectrum, given in Fig. 2(a), shows that the extra structure is shifted by 5.1 eV to the higher kinetic energy side from the main Auger peak. The new structure is fitted using only one peak corresponding to the ^1D line. The ^1S Auger peak is not included, as it is strongly overlapping with much more intense peaks. In order to reach a reasonable fit we had to include the third peak which was observed to be separated by 2.4 eV from the main peak. In the case of KL_1L_{23} and KL_1L_1 Auger transitions the shifts between the main and new peaks were found to be 4–5 eV. The fit of the KL_1L_{23} spectrum is presented in Fig. 3(a). Note that the intensity of the KL_1L_{23} group is much lower than that of the $KL_{23}L_{23}$ group and distributed between ^1P and ^3P lines, as can be seen from Fig. 1. This and the overlapping Li 1*s* photoline limit strongly the accuracy of the fit. The group has also a tail on its high kinetic energy side, containing satellite lines which result most probably from the $KL_{23}L_{23}$ Auger transitions in the presence of an addi-

TABLE I. Experimental absolute and relative energies (in eV) for the $KL_{23}L_{23}(^1D)$ lines.

Line	Spectrum	E_{kin}	ΔE_{kin}
LiF			
normal	*N* in Fig. 1	653.6	
main	Fig. 2(a)	654.2	0.6
main	Fig. 2(b)	654.7	1.1
3*p*	Fig. 2(a)	659.3	5.7
4*p*	Fig. 2(b)	657.7	4.1
$3p \rightarrow 4p$	Fig. 2(a)	656.6	3.0
$4p \rightarrow 3p$	Fig. 2(b)	660.2	6.6
NaF			
normal	*N* in Fig. 4	653.6	
main	Fig. 5(a)	654.4	0.8
main	Fig. 5(b)	654.5	0.9
3*p*	Fig. 5(a)	658.1	4.5
4*p*	Fig. 5(b)	657.2	3.6
KF			
normal	*N* in Fig. 6	656.2	
main	Fig. 7(a)	656.6	0.4
main	Fig. 7(b)	656.5	0.3
3*p*	Fig. 7(a)	659.1	2.9
4*p*	Fig. 7(b)	658.6	2.4

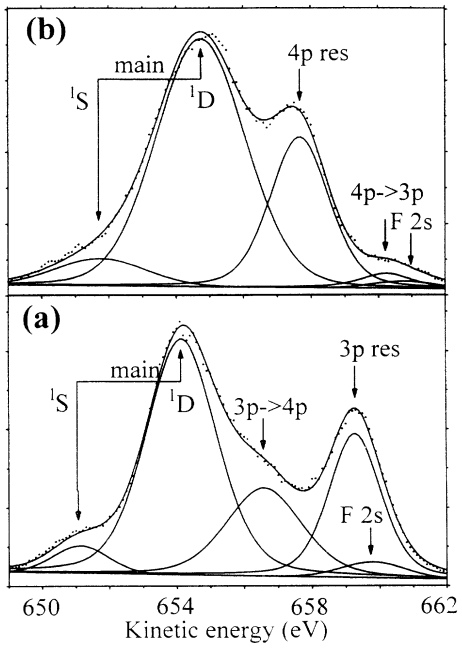

FIG. 2. (a) F $KL_{23}L_{23}$ resonant Auger spectrum of LiF taken at the mean photon energy *b* of Fig. 1, decomposed into the line componets. Fluorine 2*s* is indicated by F 2*s*. For other notations see Sec. III B. (b) F $KL_{23}L_{23}$ resonant Auger spectrum of LiF taken at the mean photon energy *d* of Fig. 1.

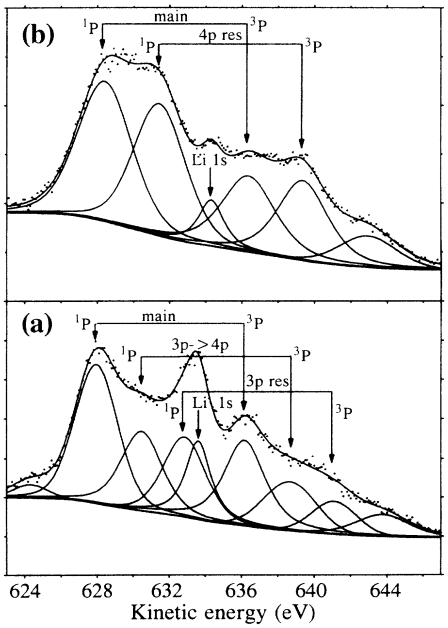

FIG. 3. (a) F KL_1L_{23} resonant Auger spectrum of LiF taken at the mean photon energy *b* of Fig. 1, decomposed into the line components. Lithium 1*s* is indicated by Li 1*s*. For other notations see Sec. III B. (b) F KL_1L_{23} resonant Auger spectrum of LiF taken at the mean photon energy *d* of Fig. 1.

tional hole in the fluorine L shell. These satellite lines were observed for Ne.[9] The satellite lines have been partially taken into account by including an extra peak at around 644 eV, although there is very probably a satellite contribution also at lower kinetic energies. The intensities and energy positions of the new peaks that appeared on the high energy side of the main ^3P peak are therefore rather unreliable. Two new peaks between ^1P and ^3P main lines can be determined more accurately. They are shifted by 2.5 and 4.9 eV from the main ^1P line.

The second region, where the anomalous behavior of the resonant Auger spectrum is clearly seen, is around the photon energy marked by d in the inset of Fig. 1. At this photon energy region additional peaks, shifted by about 3 eV to higher kinetic energies, appear clearly in the electron spectra next to the main KL_1L_1, KL_1L_{23}, and $KL_{23}L_{23}$ Auger peaks. A detailed fit of the $KL_{23}L_{23}$ spectrum is presented in Fig. 2(b) and of the KL_1L_{23} spectrum in Fig. 3(b). The difficulties in fitting the KL_1L_{23} group are the same as described before. Additional peaks, shifted about 3 eV to the high kinetic energy side from the main lines, are definitely present, however.

The spectrum marked by c in Fig. 1 has no clear extra peak structure but a strong high kinetic energy tail. Keeping in mind the bandwidth of exciting photons this spectrum is obviously a superposition of the spectra marked by b and d.

The F $2s$ photoline overlaps with the resonance $KL_{23}L_{23}$ and Li $1s$ photoline with KL_1L_{23} Auger features. The positions and shapes of the photolines were fixed according to the recordings below the resonance so that their kinetic energy varied linearly with the photon energy through the resonance region. The intensity of the F $2s$ photoline is not resonating strongly as can be seen from Figs. 2(a) and 2(b).

B. NaF

The absorption maximum around 690.2 eV in the spectrum of NaF (inset of Fig. 4) is broad and structureless. The shoulder seen by Nakai *et al.*[7] is smeared out due to the moderate resolution.

The deexcitation electron spectra of NaF (Fig. 4) have been recorded at photon energies indicated by arrows a–d in the inset. The normal Auger electron spectrum recorded at $h\nu = 800$ eV is also shown in the figure. The kinetic energy region of the $KL_{23}L_{23}$ Auger transitions is presented in more detail in Figs. 5(a) and 5(b) for the spectra labeled by a and c in Fig. 4. The fits in Figs. 5(a) and 5(b) display similar extra structures as in LiF. They are shifted by about 4 eV [Fig. 5(a)] and 2.7 eV [Fig. 5(b)] to higher kinetic energies from the main Auger electron lines. Due to the heavy overlap with the Na $2p$ and F $2s$ photolines the accuracy in the determination of resonance structures is not as good as for LiF. We were not able to include a third spectral component in the fits as we did for LiF since it would have been overlapping heavily with the F $2s$ photoline. The branching ratio of the Na $2p$ and F $2s$ photolines is different in Figs. 5(a) and

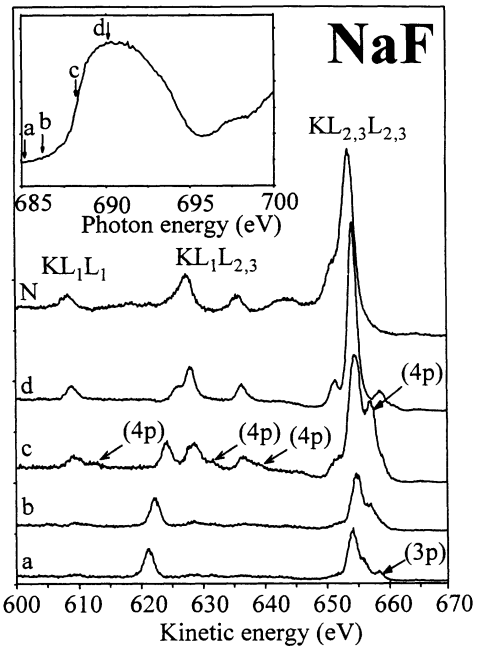

FIG. 4. Normal (denoted by N) and resonant Auger spectra of NaF recorded at photon energies shown by a–d in the inset, which depicts the total electron yield spectrum of NaF at the F K edge.

5(b), but this may be due to the inaccuracy in the decomposition procedure rather than any physical reason.

Similar extra structures can be seen also in the regions of KL_1L_1 and KL_1L_{23} Auger transitions, although the low intensity of the spectrum a (Fig. 4) reduces the accuracy of fit and disables the exact determination of line

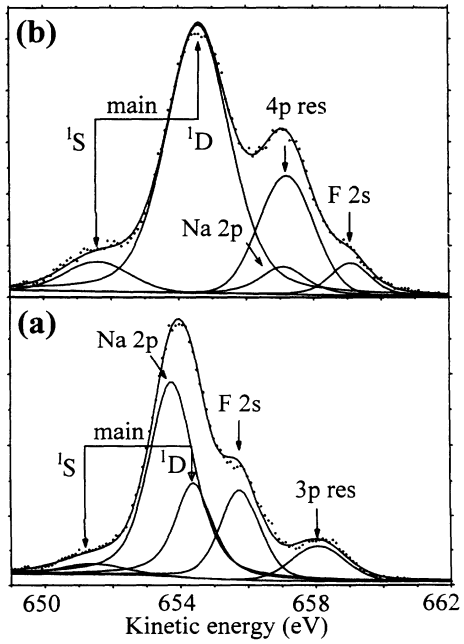

FIG. 5. (a) Decomposition of the NaF $KL_{23}L_{23}$ resonant Auger spectrum a of Fig. 3 into the line components. (b) Decomposition of the resonant Auger spectrum c of Fig. 3.

shifts. In the spectrum *c* the shift was found to be 2.7 eV for the KL_1L_{23} structure.

C. KF

The photon energy range around the first absorption maximum at 689.0 eV of KF, shown as the inset of Fig. 6, was studied by recording the electron spectra at photon energies indicated by the arrows *a*–*d*. The spectra and the normal Auger electron spectrum taken at $h\nu = 750$ eV are plotted in Fig. 6.

The main ^1D peak of the $KL_{23}L_{23}$ Auger spectrum of KF has been observed to be split into two peaks of almost equal intensity also in earlier studies.[10,11] From the fit of normal Auger electron spectrum (N) in Fig. 6 we found the branching ratio of these peaks, separated by 2.5 eV, to be almost 1:1, which is in good agreement with earlier findings. A ^1S peak is observable at the low energy side of the split main peak, separated by 2.0 eV from the nearest peak. Possible splitting of this peak remains uncertain due to intense ^1D lines nearby. Spectra *a* and *b* show distinct extra peaks in the high energy side of the main peaks. During the fitting procedure [Figs. 7(a) and 7(b)] we used an analogous triplet structure as in the normal Auger electron spectrum for the main feature but only single peaks for the resonance features. Since the intensity distribution thus obtained for the main lines completely differs from that observed for the normal Auger electron spectrum (N), the resonance features may also be composed of several peaks. Due to the heavy overlap of the resonance and main Auger peaks and the K 3*s* and F 2*s* photopeaks it was not meaningful to include more peaks in the fit, however.

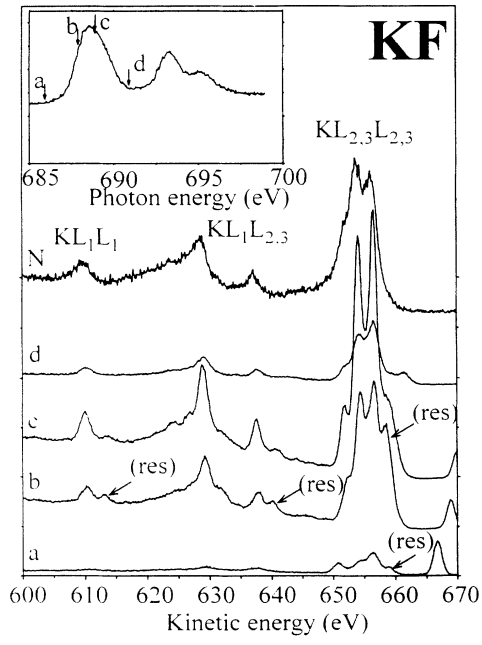

FIG. 6. Normal and resonant Auger spectra of KF. The inset depicts the total electron yield spectrum of KF at the F K edge.

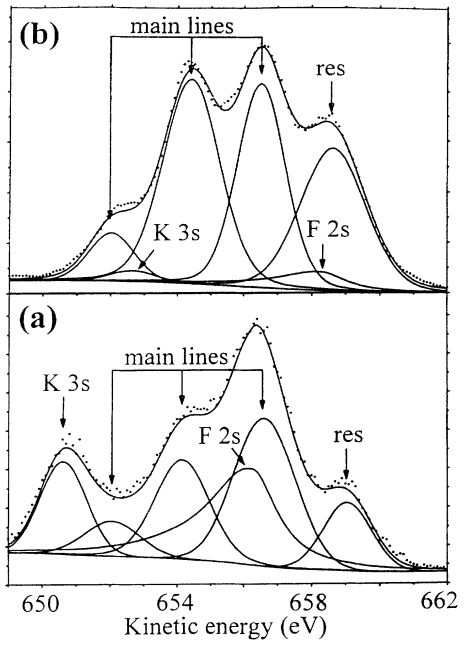

FIG. 7. (a) Decomposition of the KF $KL_{23}L_{23}$ resonant Auger spectrum *a* of Fig. 5. (b) Decomposition of the resonant Auger spectrum *b* of Fig. 5.

The KL_1L_{23} lines of spectrum *a* (Fig. 6) were too weak to be analyzed. The KL_1L_1 and KL_1L_{23} groups of spectrum *b* display similar features as the $KL_{23}L_{23}$ group.

III. DISCUSSION

Resonant Auger spectra of F discussed above display very obviously similar features as reported earlier for the Ne KLL resonant Auger spectrum.[5] This is also easy to understand since the F^- ion is isoelectronic with the Ne atom. Before discussing the fluorine spectra in more detail we shall present a short summary of the Ne results obtained on the basis of atomic multiconfiguration Dirac-Fock (MCDF) calculations.[5]

A. Calculated normal and resonant Auger spectra of Ne

Figure 8 shows the calculated resonant Auger spectra due to the $1s^13p \rightarrow (2s2p)^63p$ and $1s^14p \rightarrow (2s2p)^64p$ transitions and the normal Auger electron spectrum $1s^1 \rightarrow (2s2p)^6$. Energy positions and intensity distributions for the profiles were obtained from the MCDF calculations,[5] but the width of the lines was chosen to be 2.2 eV in order to arrive at a better resemblance with the recorded fluorine spectra.

Calculated kinetic energies for the most intense $KL_{23}L_{23}(^1D)$ line are given in the lower part of Table II for the transitions of Fig. 8. Since the shakeup of the spectator electron was observed to play a prominent role in the resonant Auger spectra of Ne,[5] Table II also shows

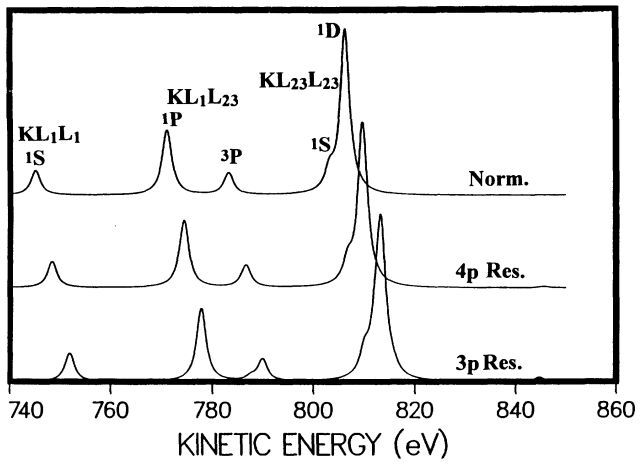

FIG. 8. Calculated normal KLL, $3p$, and $4p$ resonant Auger spectra of Ne.

the energies of the transitions where the $3p/4p$ electron has shaken up or down during the Auger decay. Energies of the shakeoff transitions are also given. Table II shows, furthermore, the energy shifts of the resonant and shake lines relative to the normal Auger lines.

Calculated energies for the photoabsorption lines and photoionization threshold of Ne are also presented in the upper part of Table II, as well as the energy differences between the first absorption maxima and the photoionization limit.

B. Assignment of fluorine resonant Auger lines

By comparing the calculated spectra of Ne with the experimental spectrum of F recorded from LiF (Figs. 1–3) the observed features can be assigned tentatively as follows: The high energy structure in Fig. 2(a) may result from spectator Auger transitions where the spectator electron has $3p$ character. We have therefore denoted the peak by "$3p$" in Figs. 1 and 2(a). The peak on its low kinetic energy side [Fig. 2(a)] could be due to the transitions where the $3p$ electron has shaken up to the $4p$ orbital during the Auger decay. In the Ne atom the branching ratio between the $3p$ spectator and $3p \rightarrow 4p$ shake transitions was found to be 2.5.[5] On the basis of the close resemblance with the behavior of the Ne results we have assigned the peak as "$3p \rightarrow 4p$" in Fig. 2(a.) The peak is somewhat broader than the "$3p$" peak. This may result from the possibility that also the $4p$ orbitals become simultaneously excited when the mean photon energy points the $3p$ resonance. The width of the $1s^1 3p$ and $1s^1 4p$ excited states may also be large enough to allow them to overlap partially. According to Table II the Ne $1s^1 4p \rightarrow 2p^4 4p$ spectator lines occur at somewhat higher kinetic energies than the $1s^1 3p \rightarrow 2p^4 4p$ shakeup lines. If both transitions take place, broadening of the peak is possible since the linewidth is too large to allow to resolve the lines.

TABLE II. Calculated absolute and relative energies (in eV) for the Ne transitions.

Initial state	Final state	E	ΔE_{absor}	ΔE_{kin}
Absorption				
$1s^2$	$1s^1$	869.4	0	
$1s^2$	$1s^1 3s$	864.6	4.8	
$1s^2$	$1s^1 3p$	866.5	2.9	
$1s^2$	$1s^1 4p$	868.1	1.3	
Auger decay				
$1s^1$	$2p^4(^1D)$	806.9		0
$1s^1 3s$	$2p^4(^1D)3s$	815.3		8.4
$1s^1 3p$	$2p^4(^1D)3p$	813.6		6.7
$1s^1 3p$	$2p^4(^1D)4p$	808.7		1.8
$1s^1 3p$	$2p^4(^1D)5p$	806.8		−0.13
$1s^1 3p$	$2p^4(^1D)$	803.9		−2.9
$1s^1 4p$	$2p^4(^1D)4p$	810.3		3.4
$1s^1 4p$	$2p^4(^1D)3p$	815.1		8.2
$1s^1 4p$	$2p^4(^1D)5p$	808.3		1.5
$1s^1 4p$	$2p^4(^1D)$	805.5		−1.4

The main peak in Fig. 2(a) has most probably a contribution from the transitions where the spectator electron has shaken up to higher orbitals during Auger decay. It may also result from transitions where the electron is originally excited to states where it is localized loosely to the fluorine ion. If the distance between the excited electron and the hole states involved in the Auger decay is increasing, the screening effect becomes weaker and only a small energy shift is observed if compared with the normal Auger spectrum excited by 800 eV photons.

Similar considerations allow us to assign the features in Fig. 3(a) also as spectator Auger transitions, the spectator electron having $3p$ character (denoted "$3p$"), and $3p \rightarrow 4p$ shakeup transitions (denoted "$3p \rightarrow 4p$"). Both ^1P and ^3P main lines have resonant peaks.

On the basis of similar arguments the strong high kinetic energy structure in Fig. 2(b) can be assigned to the $4p$ spectator Auger transitions. Weak structure on its high energy side may contain, in addition to the F $2s$ photoline, also transitions where the excited electron shakes down to the $3p$ during the Auger decay. In Ne the shakeup transitions to higher orbitals were found to be important.[5] The main peak of Fig. 2(b) may thus result from a superposition of shakeup transitions and transitions where the excited electron is originally loosely bound to the core hole. The broadening of the ^1D peak in passing from Fig. 2(a) to 2(b) indicates that shakeup transitions play an important role in Fig. 2(b). Note also that the ^1S component of the "$4p$" transitions overlaps with the ^1D main line.

The $4p$ spectator structure is found also in Fig. 3(b). The broadening of main lines seems also to occur while passing from Fig. 3(a) to Fig. 3(b).

The findings for NaF and KF are in a good agreement with the results for LiF. In both cases it is possible to identify a spectator Auger contribution in the spectra when the photon energy is tuned to the shoulder of the absorption maxima. In LiF and NaF the behavior of resonances closely follows that observed for an isoelectronic Ne atom, and characterization to the "3p" and "4p" reso-

nances seems to be justified. The normal Auger electron spectrum of KF, on the other hand, is not characterized by a pure atomic multiplet structure but shows features where the electrons involved in the Auger decay originate from a molecular orbitallike state between the metal and the fluorine ion.[10,11] In this case the characterization of the exciton state by an atomlike orbital nomenclature is not meaningful any more. This is also supported by the observation that the highest kinetic energy main line is much more intense [Figs. 7(a) and 7(b)] than the corresponding line in the normal Auger electron spectrum (N) thus indicating that it also contains a contribution from the resonant spectrum.

Localized excitonic states seem to appear, according to the present study, in all the alkali fluorides. Delocalized excitons would not be able to produce as large kinetic energy shifts of resonant Auger lines as observed now. The shifts were found to be of the same order of magnitude as detected earlier for Ne.[5] According to Tables I and II the first resonant spectra were found to shift from the normal Auger spectrum by 6.7 eV, 5.7 eV, 4.5 eV, and 2.9 eV in Ne, LiF, NaF, and KF, respectively. The shifts for the second resonance spectra were found to be 3.4 eV, 4.1 eV, 3.6 eV, and 2.4 eV. Since the participator decay was not significant for Ne it most probably is not important in fluorine either.

All the resonant spectra seem to have a peak labeled by "main" in Figs. 2, 5, and 7. This is assumed to contain a contribution from the decay of excited states with loosely bound electrons that causes a weak screening effect. The peak appears simultaneously with the peak resulting from the localized "3p" exciton already when the resonant Auger structure begins to become apparent. We were able to fit the peak with a symmetric line shape which indicates that it is of resonant character since PCI (post collision interaction) produces asymmetric line shapes. The peak was found to appear at about 1 eV higher kinetic energy than the normal Auger electron line excited by 800 eV photons. Its position was found to vary slightly at different photon energies around the threshold. Possible charging effects and large linewidths make the fitting somewhat inaccurate and therefore we were not able to determine the energy dependence of the main peak on the photon energy.

All the Auger spectra recorded in the vicinity of the absorption maxima (spectrum e in Fig. 1, d in Fig. 4, and c in Fig. 6) seem to differ distinctly from the normal Auger electron spectrum taken at $h\nu = 800$ eV. The spectra appear at about the same kinetic energies as the main lines in the spectra taken below the absorption maxima and they also display narrow linewidths. This indicates the existence of a pronounced screening effect. Only the spectrum d in Fig. 6 starts to resemble the normal Auger spectrum recorded far from threshold.

C. Linewidths

The linewidths of the normal and resonant Auger spectra seem to differ considerably. The widths of the normal Auger electron lines recorded at $h\nu = 800$ eV are about twice as large as those of "3p" and "4p" resonant Auger lines. The inherent widths of the Auger lines originate from the lifetime width resulting from electronic transitions and solid-state broadening which is a combination of vibrational (phononic) and dispersional broadenings.[12,13] The observed spectrum is further broadened by the electron spectrometer. In the present case this is, however, a minor factor.

The lifetime width of the 1s core hole of Ne is only 0.2 eV.[5] Because of the small lifetime width the PCI shifts and asymmetries were found to be very small in the Ne atom.[5] The normal and resonant Auger decay rates of Ne were found to differ only slightly.[5] The Auger decay rate is determined by the wave functions of the electrons involved in the decay. Atomlike behavior has now been observed for the normal and resonant Auger spectra of studied ionic solids indicating that the wave functions retain a great deal of their atomic character. The lifetime widths due to the electronic transitions for the fluorine 1s core hole state may thus not differ considerably from Ne.

When the electronic state of an atom in a solid is changed the atomic equilibrium positions are altered. The lattice cannot relax during the very short time period of the electronic transition. This results in the creation of phonons in the final state of the transition which leads to the broadening of the spectral lines.[13] Since the equilibrium positions depend on the electronic state the amount of phonon relaxation may differ for transitions between different electronic states manifesting itself as changed linewidths.

The possibility of dispersional broadening is related to the amount of hybridization. The larger hybridization results in larger bandwidths in the solid state. The dispersion can be reduced by excitonic effects where the larger core-hole attraction localizes the electron.[12] Decrease of the dispersional broadening in the localized excitonic states of fluorides might explain the observed decrease of the "3p" and "4p" resonant Auger linewidths.

If the excited states are broadened by the solid-state effects but the photon bandwidth is narrower than the width of the excited state, the Auger resonant Raman effect[14] becomes possible. The width and shape of the Auger lines follow then that of the photon beam. Our absorption spectra do not display features detected earlier by high resolution measurements,[7] indicating that the width, e.g., of the first exciton may not be larger than the bandwidth used. Further measurements with varying bandwidths are, however, needed to clarify this point.

D. Features of photoabsorption spectra

The analyzed resonant Auger spectra reveal valuable additional information for the understanding of the photoabsorption spectra. The spectra of fluorides with different cations are quite dissimilar and their detailed understanding has been lacking for the time being. Nakai *et al.*[7] calculated the photoabsorption of LiF and NaF using a short-range multiple scattering approach and got satisfactory agreement in peak positions, but did not succeed

to reproduce the shoulders below the first strong peak. The problem in reproducing the absorption structure below or near the edge confirms our findings of the existence of different localized states in this energy region.

The mean excitation energies for the observed two different localized final states, obtained from the comparison of the resonant Auger and photoabsorption spectra, are quite similar for NaF (685.2 and 688.2 eV) and KF (685.7 and 688.2 eV), but are clearly higher for LiF (690.5 and 691.7 eV). Note that also the photoabsorption maxima are shifted from 689.0 eV to 690.2 eV and 692.5 eV while passing from KF to NaF and LiF, respectively. In the absorption spectrum of Ne the energy difference between the $1s^1 2s^2 2p^6 3p$ and $1s^1 2s^2 2p^6 4p$ final states is 1.6 eV,[15,16] being of the same order of magnitude as the difference between the localized excitation in LiF and slightly smaller than in NaF and KF. The photoabsorption cross section for the Ne $1s \rightarrow 3p$ excitation is 2.5 times stronger than for the $1s \rightarrow 4p$ excitation. In alkali fluorides the higher energy localized state was observed to have higher intensity than the lower energy localized state. This is seen as the increase of the intensity of the deexcitation spectra in passing from the first to the second resonance. Based on the intensity ratio of the resonance absorptions, an alternative explanation to the nomenclature of the excitons as "$3p$" and "$4p$" could be that the low energy localized state is due to the $3s$ state of F or due to the s state of metal origin. Such transitions are forbidden in atoms, but may be allowed in solids. A similar explanation was used earlier to explain the feature below the $1s^1 2p^1$ final state in the Li K absorption spectra of LiF as a "forbidden" $1s^2 \rightarrow 1s^1 2s^1$ transition.[17] In this case the localized high energy state could correspond excitations to the $3p$-like orbital.

In the Ne atom the energy difference between the $1s^1 3s$ excited state and $1s^1$ ionized state is 4.8 eV according to Table II and the $1s^1 3s \rightarrow 2p^4 3s$ transitions are shifted by 8.4 eV from normal Auger transitions. If the first localized state of fluorides is of $3s$ origin, the energy shifts are considerably decreased from the corresponding ones in the Ne atom. This is naturally possible since the chemical and solid-state effects are strong in these crystals and may have considerable influence to the atomic picture used. In order to reach a complete understanding of the nature of the excitons, extended calculations including solid-state effects are needed.

IV. CONCLUSIONS

The resonant Auger spectra of F measured from LiF, NaF, and KF have been used to study the nature of the F core excitons. Broad structureless absorption peaks have been identified by comparing with the results for the isoelectronic Ne atom to contain regions with two different excitonic states, one of them being obviously of $3p$ and another of $4p$ atomic character.

Additionally we have observed a significant narrowing of the halfwidths of the Auger lines resulting from the decay of excitons. This is assumed to be related to the localization of the excited electron in the presence of an attractive core hole removing to a large extent the solid-state broadening.

ACKNOWLEDGMENTS

These investigations have been supported financially by the Research Council for the Natural Sciences of the Academy of Finland. The University of Oulu, the Academy of Finland, and the Swedish Institute are acknowledged for providing Financial support for E. Kukk, A. Kikas, and A. Ausmees, respectively. The authors would like to thank the staff of the MAX laboratory for their assistance with the beam line 22 and the opportunity to use its experimental setup.

* Permanent address: Institute of Physics, Estonian Academy of Sciences, Riia 142, EE2400 Tartu, Estonia.

[1] H. Aksela, M. Bancroft, and B. Olsson, Phys. Rev. A **46**, 1345 (1992).
[2] T. Tiedje, K. M. Colbow, D. Rogers, and W. Eberhardt, Phys. Rev. Lett. **65**, 1243 (1990).
[3] M. Elango, A. Ausmees, A. Kikas, E. Nõmmiste, R. Ruus, A. Saar, J. F. van Acker, J. N. Andersen, R. Nyholm, and I. Martinson, Phys. Rev. B **47**, 11736 (1993).
[4] H. Aksela, S. Aksela, A. Mänttykenttä, J. Tulkki, E. Shigemasa, A. Yagishita, and Y. Furusawa, Phys. Scr. T **41**, 113 (1992).
[5] H. Aksela, S. Aksela, J. Tulkki, T. Åberg, G. M. Bancroft, and K. H. Tan, Phys. Rev. A **39**, 3401 (1989).
[6] J. N. Anderson, O. Björneholm, A. Sandell, R. Nyholm, J. Forsell, L. Thånell, A. Nilsson, and N. Mårtensson, Sync. Radiat. News **4**, 15 (1991).
[7] S. Nakai, M. Ohashi, T. Mitsuishi, H. Maezawa, H. Oizumi, and T. Fujikawa, J. Phys. Soc. Jpn. **55**, 2436 (1986).
[8] C. Sugiura, J. Phys. Soc. Jpn. **60**, 1406 (1991).
[9] M. Leväsalmi, H. Aksela, and S. Aksela, Phys. Scr. T **41**, 119 (1992).
[10] O. Benka and M. Uda, Phys. Rev. Lett. **56**, 1667 (1986).
[11] D. S. Urch, J. Chem. Soc. Chem. Commun. **1982**, 526 (1982).
[12] F. M. F. de Groot, J. C. Fuggle, B. T. Thole, and G. A. Sawatzky, Phys. Rev. B **41**, 928 (1990).
[13] W. L. O'Brien, J. Jia, Q.-Y. Dong, T. A. Callcott, D. R. Mueller, and D. L. Ederer, Phys. Rev. B **45**, 3882 (1992).
[14] G. S. Brown, M. H. Chen, B. Crasemann, and G. E. Ice, Phys. Rev. Lett. **45**, 1937 (1980).
[15] A. P. Hitchcock and C. E. Brien, J. Phys. B **13**, 3269 (1980).
[16] J. M. Esteva, B. Gauthe, P. Dhez, and R. C. Karnatak, J. Phys. B **16**, L263 (1983).
[17] B. F. Sonntag, Phys. Rev. A **9**, 3601 (1974).